

ARTICLE



IMMUNOTHERAPY

Inserting EF1 α -driven CD7-specific CAR at CD7 locus reduces fratricide and enhances tumor rejection

Jie Jiang^{1,2,3}, Jiangqing Chen^{1,2,3}, Chan Liao⁴, Yanting Duan^{1,2,3}, Yajie Wang^{1,2,3}, Kai Shang^{1,2,3}, Yanjie Huang⁵, Yongming Tang⁴, Xiaofei Gao⁵, Ying Gu^{2,6,7,8} and Jie Sun^{1,2,3}

© The Author(s), under exclusive licence to Springer Nature Limited 2023

CAR-T therapies to treat T-cell malignancies face unique hurdles. Normal and malignant T cells usually express the same target for CAR, leading to fratricide. CAR-T cells targeting CD7, which is expressed in various malignant T cells, have limited expansion due to fratricide. Using CRISPR/Cas9 to knockout CD7 can reduce the fratricide. Here we developed a 2-in-1 strategy to insert EF1 α -driven CD7-specific CAR at the disrupted CD7 locus and compared it to two other known strategies: one was random integration of CAR by a retrovirus and the other was site-specific integration at T-cell receptor alpha constant (*TRAC*) locus, both in the context of CD7 disruption. All three types of CD7 CAR-T cells with reduced fratricide could expand well and displayed potent cytotoxicity to both CD7⁺ tumor cell lines and patient-derived primary tumors. Moreover, EF1 α -driven CAR expressed at the CD7 locus enhances tumor rejection in a mouse xenograft model of T-cell acute lymphoblastic leukemia (T-ALL), suggesting great clinical application potential. Additionally, this 2-in-1 strategy was adopted to generate CD7-specific CAR-NK cells as NK also expresses CD7, which would prevent contamination from malignant cells. Thus, our synchronized antigen-knockout CAR-knockin strategy could reduce the fratricide and enhance anti-tumor activity, advancing clinical CAR-T treatment of T-cell malignancies.

Leukemia; <https://doi.org/10.1038/s41375-023-01948-3>

INTRODUCTION

Chimeric antigen receptor (CAR) T cell therapy is a significant breakthrough in cancer treatment, having produced remarkable clinical responses in refractory or relapsed B-cell malignancies and multiple myeloma by targeting CD19 and BCMA [1–3]. However, the extended application of CAR-T therapy to T-cell malignancies remains challenging [4]. A major obstacle is the shared expression of many targetable antigens between normal and malignant T cells, which can cause fratricide in CAR-transduced T cells, inhibiting their expansion, such as CD3, CD5, and CD7.

Targets for CAR-based immunotherapy to treat T-cell malignancies include CD5, CD4, CD30, CD7, etc [4]. CD7 is a transmembrane glycoprotein of the immunoglobulin supergene family, mainly expressed by T cells, NK cells and their precursors [5]. It is one of the earliest markers for human T cell lineage thus immunotherapy targeting CD7 can cover most kinds of T-cell malignancy subtypes including early T-cell precursor lymphoblastic leukemia, which is a high-risk subset accounting for ~10–13% of pediatric and 5–10% of adult T-ALL cases [6]. CD7 as an attractive

target of immunotherapy has been studied for decades. While preclinical studies of CD7 antibodies and ADCs have reported promising anti-T-ALL potential [7–11], no such products are currently available in the clinic. Standard therapy for T-ALL is intensive combination chemotherapy, and allogeneic hematopoietic cell transplantation still plays a key role in patients with high-risk or relapsed/refractory disease [12, 13]. However, 5-year survival is <75% for children and <50% for adults [13]. Innovative therapies are urgently needed for the treatment of T-cell malignancies. Now over ten CD7 CAR-T cell therapies are being tested in clinical trials, mainly to treat T-cell leukemia and T-cell lymphoma (NCT05212584, NCT04934774, NCT05059912, NCT04823091, NCT04840875, NCT05290155, NCT04689659, etc.) [14, 15]. Early results from a single-center first-in-human phase I trial have shown a high complete remission rate with a manageable safety profile of CD7 CAR-T cells [16, 17]. However, preclinical studies reported impaired CD7 CAR-T cell expansion resulting from fratricide [18]. Similar drawback also exists in several other CAR-T cells targeting T-cell malignancies, such as CD3 and CD5 CAR-T cells [19, 20]. To

¹Bone Marrow Transplantation Center of the First Affiliated Hospital and Department of Cell Biology, Zhejiang University School of Medicine, 866 Yuhangtang Road, Hangzhou 310058, China. ²Liangzhu Laboratory, Zhejiang University Medical Center, 1369 West Wenyi Road, Hangzhou 311121, China. ³Institute of Hematology, Zhejiang University & Zhejiang Engineering Laboratory for Stem Cell and Immunotherapy, Hangzhou 310058 Zhejiang, China. ⁴Department of Hematology-oncology, Children's Hospital, Zhejiang University School of Medicine, Hangzhou, Zhejiang, China. ⁵Key Laboratory of Structural Biology of Zhejiang Province, School of Life Sciences, Westlake University, Hangzhou 310058, China. ⁶Cancer Institute (Key Laboratory of Cancer Prevention and Intervention, China National Ministry of Education), the Second Affiliated Hospital, Zhejiang University, School of Medicine, Hangzhou, Zhejiang 310009, China. ⁷Institute of Genetics, Zhejiang University and Department of Genetics, Zhejiang University, School of Medicine, Hangzhou 310058, China. ⁸Zhejiang Provincial Key Lab of Genetic and Developmental Disorder, Hangzhou, Zhejiang 310058, China. [✉]email: guyinghz@zju.edu.cn; sunj4@zju.edu.cn

Received: 11 October 2022 Revised: 5 June 2023 Accepted: 15 June 2023

Published online: 30 June 2023

rescue cell expansion, using gene editing to disrupt the target is now the mainstream approach [18, 20–23]. Some alternative ways, such as blocking CD7 protein trafficking to the cell surface or engineering naturally CD7-negative subtype of T cells [24, 25], could also reduce fratricide.

Current FDA-approved CAR-T products are manufactured using retroviral or lentiviral vectors [26], which integrate CARs in a semi-random fashion and may result in unexpected disruption of normal genes [27]. A previous study reported that targeting a CD19 CAR specific to the T-cell receptor alpha constant (*TRAC*) locus using CRISPR/Cas9 could make CAR-T cells outperform retrovirus-transduced ones [28]. Additionally, long-term lentiviral vector integration site analysis of CAR-T cells sorted from patient's blood showed that CAR insertions into different gene sites emerged at different time points and some of them have advantages on stabilization or abundance of CAR-T cell clones [29]. It suggests that the integration site of CAR may affect CAR-T cell proliferation and differentiation. Since the *CD7* locus needs to be disrupted to reduce fratricide in CD7 CAR-T cells, we explore whether we could take advantage of this abandoned locus as a recycled site to express CD7 CAR. Thus, we develop a 2-in-1 strategy to knockout (KO) CD7 and knockin (KI) CD7 CAR simultaneously by inserting CD7 CAR directly to the *CD7* locus. Our results have showed that this strategy not only reduces the fratricide of CD7 CAR-T cells but also enhances tumor rejection compared to retrovirus-transduced cells. Using CAR-NK cells instead of CAR-T cells to treat T-ALL can avoid malignant T cell contamination, but NK cells also express CD7 leading to fratricide [5]. So, we applied the same 2-in-1 strategy to generate CD7-specific CAR-NK cells and tested their in vitro and in vivo functions.

RESULTS

Potent cytotoxicity coincided with fratricide of CD7 CAR-T cells

The antigen recognition domain largely influences CAR-T efficacy as it provides the most upstream signal for CAR-T activation. We chose three single-chain variable fragments (scFvs) derived from different CD7-specific antibody clones (No. T3-3A1, 3A1F, TH69) to construct CD7 CARs (Fig. 1A). In our design, three scFvs were separately cloned into a second-generation CAR backbone containing CD28 and CD3 ζ endodomains, followed by a P2A self-cleavage peptide and an enhanced green fluorescence protein as the reporter gene to estimate CAR expression. Transduction of primary human T cells with γ -retrovirus resulted in efficient expression of all three CD7 CARs (Fig. 1B). Using the leukemic T-cell line Jurkat cells as targets (Fig. S1A), we compared their cytotoxic effects by in vitro killing assay. Both 3A1F and TH69 CAR-T cells displayed much higher cytotoxic effects than T3-3A1 CAR-T cells, which showed minimal cytotoxicity close to untransduced T cells (Fig. 1C). This result was confirmed in another donor (Fig. S1B). Next, we analyzed the cytokine release of CAR-T cells by the Human Inflammatory Cytokine Cytometric Bead Array (CBA) Kits. Similarly, both 3A1F and TH69 CAR-T cells secreted much higher IFN- γ , TNF- α , and IL-2 than T3-3A1 CAR-T cells upon antigen stimulation (Fig. 1D). T3-3A1 antibody has shown specific binding to CD7⁺ T cells and has long been explored as a candidate for T cell probes and ADCs [9, 30]. Nevertheless, CAR construct using T3-3A1 scFv as antigen recognition domain cannot effectively activate CAR-T cells to secrete cytokines and kill target cells.

In previous studies, CD7-specific CAR expression by lentiviral or retroviral transduction induced fulminant T-cell fratricide which is caused by self-recognition of CAR-T cells due to the shared expression of CD7 between them and malignant T cells [18]. Herein, we first confirmed high CD7 expression on primary human T cells (Fig. 1E). Compared to T3-3A1 CAR-T cells, both 3A1F and

TH69 CAR-T cells have lower cell viability (Fig. 1F) and reduced long-term cell proliferation (Fig. 1G), suggesting that these two CD7-specific CAR-T cells could kill CD7⁺ CAR-T cells causing fratricide and their higher cytotoxicity against target tumor cells coincided with their higher fratricide. The same trend could also be observed in a different donor (Fig. S1C, D). To summarize, 3A1F and TH69 CAR-T cells showed potent cytotoxicity and robust cytokine secretion upon target stimulation but failed to expand ex vivo due to fratricide. Therefore, disrupting the surface expression of CD7 on T cells to prevent fratricide is required for CD7 CAR-T cell production. In addition, we chose TH69 CARs for the following studies as TH69 CAR-T cells secreted more IL-2 (Fig. 1D) and an HA tag was added at the N-terminal of the TH69 scFv to enable direct CAR detection.

A 2-in-1 strategy to produce CD7 CAR-T cells with robust expansion

To reduce fratricide, previous studies abrogated CD7 and CAR binding either by blocking CD7 protein trafficking to the cell surface or knocking out CD7 with CRISPR/Cas9 [18, 21, 24]. These strategies reduced fratricide and allowed cell expansion without affecting the cytotoxicity of CD7 CAR-T cells. However, all these CD7 CAR-T cells were produced using lentivirus or retrovirus, which inserted CAR genes into the genome in a semi-random manner. Eyquem et al. have recently shown that inserting a CD19 CAR into the *TRAC* locus by CRISPR/Cas9 reduces CAR-mediated tonic signaling and enhances tumor rejection [28]. Therefore, we investigated whether inserting a CD7 CAR into the *TRAC* locus would be better than introducing a CD7 CAR by retrovirus both in the context of CD7 disruption to avoid fratricide. We first confirmed that the knockout efficiency of a reported CD7 gRNA targeting the second exon of *CD7* locus [18] could reach 80–90% (Fig. S2A, B) and generated CD7^{KO}RV CAR-T cells (Figs. 2A, B, S3A). Combined with a reported *TRAC* gRNA targeting the first exon of *TRAC* locus [28], the double knockout efficiency could reach more than 80% (Fig. S2C). Next using both gRNAs and an adeno-associated virus (AAV) vector repair matrix coding a P2A followed by a CD7 CAR, we generated CD7^{KO}TRAC^{KI} CAR-T cells (Fig. 2A, B, S3B). However, this strategy required two gRNAs, which would increase both the off-target risk and the cost. Thus, we designed a 2-in-1 strategy-CD7^{KO&KI} to insert the CD7 CAR gene directly into the *CD7* locus (Fig. 2A, B, S3C), resulting in CD7 knockout to reduce fratricide and simultaneous CD7 CAR expression from this disrupted locus. To ensure constant CAR expression, the exogenous promoter EF1 α was used to drive CAR expression, and the products were named as CD7^{KO&KI}EF1 α CAR-T cells (Fig. 2A). In this way, synchronous target knockout and CAR knock-in can be effectuated.

All three strategies resulted in high percentages of CAR⁺ CAR-T cells, but with different CAR expression levels (Fig. 2C). The CAR mean fluorescent intensity (MFI) of TRAC^{KI} CAR-T was significantly lower than RV CAR-T cells, consistent with previous results observed in the CD19 CAR scenario (Fig. 2C) [28]. Genome PCR results confirmed that the CAR sequence was successfully integrated into our designed *TRAC* and *CD7* loci, respectively (Fig. S4). The disruption of CD7 expression significantly improved cell viability and enabled continuous cell expansion of all three types of CAR-T cells (Fig. 2D, E, S5A, B). The total cell number of CAR-T cells expanded about 10–30 times among different donors within a week (Fig. 2E, S5B). Noticeably, the viability of CAR-T cells was slightly lower on Day3 than that of cells from Day5 and Day7, which is possibly due to electroporation-induced cellular injury and residual CD7-triggered fratricide as it was hard to achieve 100% knockout efficiency of CD7. Nevertheless, the viability and expansion were much better than CAR-T cells without CD7 knockout (Fig. 1G), indicating our strategies of making CD7^{KO} CAR-T cells limited fratricide and enabled robust cell expansion.

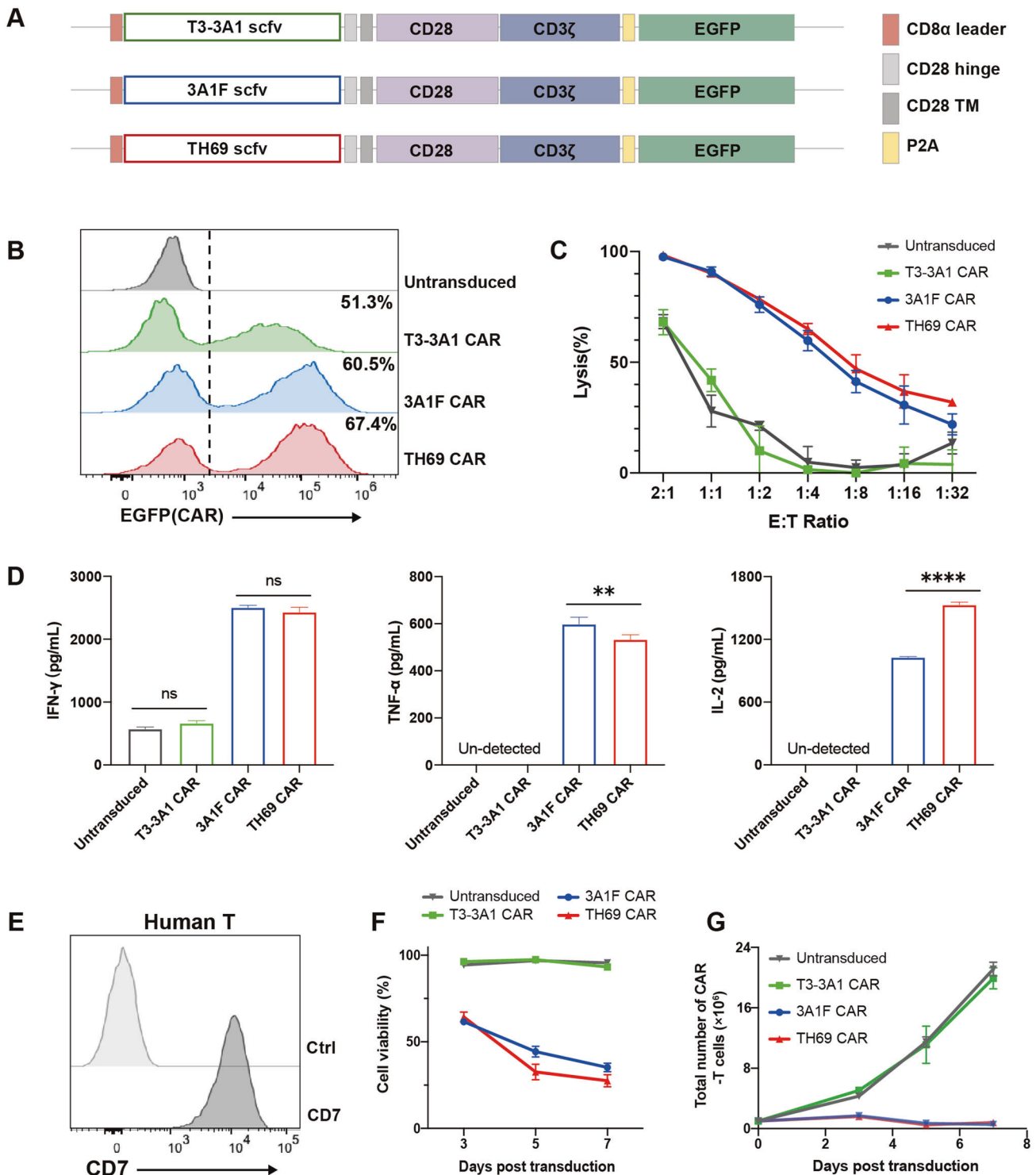


Fig. 1 Potent cytotoxicity coincided with fratricide of CD7 CAR-T cells. **A** Constructions of CD7-specific second-generation CD28-based CARs with different scFvs following an EGFP as the reporter gene. **B** Representative histogram showing CAR expression in CAR-T cells. **C** Cytotoxicity assay of indicated CAR-T cells against Jurkat cells ($n = 3$, mean \pm s.d.). **D** CAR-T cells were co-cultured with Jurkat cells for 24 h. The cytokine secretion in the supernatant was evaluated using CBA kit and FACS ($n = 3$, mean \pm s.d.). **E** Representative histogram showing surface expression of CD7 in human T cells. Ctrl, unstrained control. **F** Representative cell viability of T cells on indicated days after CAR transduction ($n = 3$, mean \pm s.d.). **G** Representative cell counts of T cells on indicated days after CAR transduction ($n = 3$, mean \pm s.d.).

Robust effector functions of three CD7^{KO} CAR-T cells in vitro

Next, we determined the effector functions of CD7^{KO} CAR-T cells. In vitro killing assay determined that three types of CAR-T had similar cytotoxicity to Jurkat cells and all of them displayed robust cytokine secretion upon target stimulation (Fig. 2F, G, S5C, D).

Summarized cytokine data from 3 donors showed no obvious difference among the three CAR-T cells (Fig. 2G). In the CFSE-based proliferation assay, we observed rapid CAR-T cell division upon target stimulation (Fig. 2H). The results also showed some of the CAR-T cells were in the division phase without any target

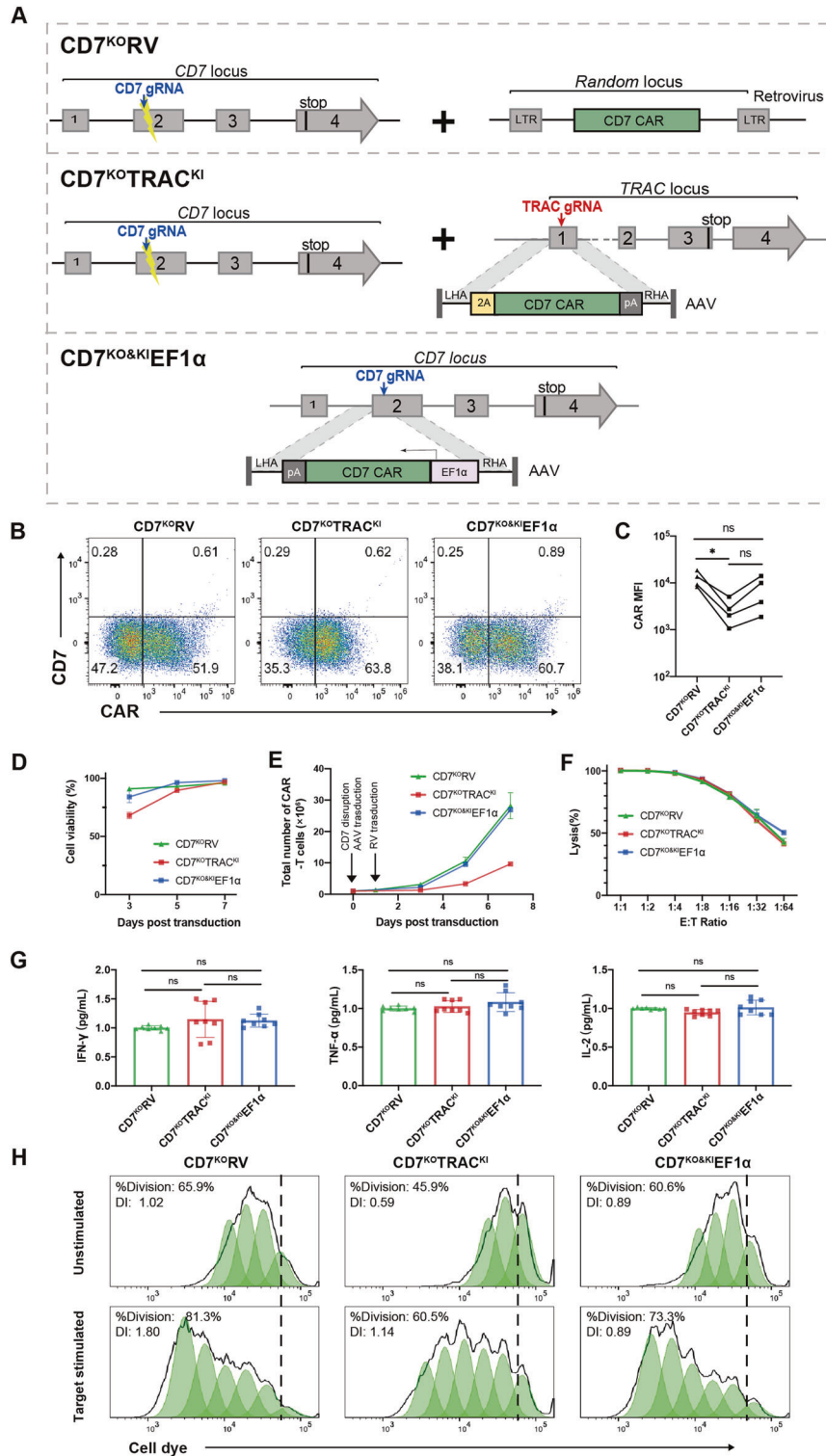


Fig. 2 A 2-in-1 strategy to produce expandable and functional CD7^{KO} CAR-T cells. **A** CRISPR/Cas9-targeted gene knockout and CAR gene integration into the genome. Top, retrovirus induced random integration of CAR and disrupted CD7 locus; middle, edited TRAC locus and disrupted CD7 locus; bottom, edited CD7 locus with 2-in-1 strategy. **B** Representative dot plots showing surface expression of CD7 and CD7-specific CAR in CAR-T cells. Numbers indicate the percentage of cells in each quadrant. **C** CAR MFI of CAR⁺ T cells ($n = 4$ independent experiments, 4 donors). **D** Representative cell viability of T cells on indicated days after CAR transduction ($n = 3$, mean \pm s.d.). **E** Representative cell counts of T cells on indicated days after CAR transduction ($n = 3$, mean \pm s.d.). **F** Cytotoxicity assay of indicated CAR-T cells against Jurkat target cells ($n = 3$, mean \pm s.d.). **G** CAR-T cells were co-cultured with Jurkat cells for 24 h. The cytokine secretion in the supernatant was evaluated using CBA kit and FACS (results from three healthy donors, $n = 8$, mean \pm s.d.). **H** Representative histograms showing cell dye dilution in CAR-T cells in the presence or absence of Jurkat cells for 96 h. Proliferation peaks were fitted by the Proliferation tool in FlowJo. Cell dye, CytoTell™ Orange.

stimulation. CD3/CD28 stimulation before CAR transduction and tonic signaling caused by CAR spontaneous aggregation could be possible reasons for this. The lower non-specific proliferation of CD7^{KO}TRAC^{KI} CAR-T cells coincides with their lower tonic signaling reported by Eyquem et al. (Fig. 2H). We used the target stimulated/unstimulated ratio of the Division Index (the average number of cell divisions that a cell in the original population has undergone) to represent antigen-induced cell division. Our results showed that this ratio of CD7^{KO}TRAC^{KI} CAR-T cells was higher than that of CD7^{KO}RV cells while the ratio of CD7^{KO&KI}EF1 α CAR-T cells was in between (Fig. S6). To further analyze CAR-T cell function, we examined T-cell phenotype after three-repeated stimulations in a one-month period (Fig. S7). Compared to CD7^{KO}RV CAR-T cells, CD7^{KO}TRAC^{KI} CAR-T cells were comprised of 2.5-fold more CD62L⁺ cells, a phenotype associated with greater *in vivo* anti-tumor activity (Fig. S7) [31]. CD7^{KO&KI}EF1 α CAR-T cells maintained this phenotype in the middle, similar to their rank regarding the CAR expression levels.

Besides T-cell leukemia, T-cell malignancies also include different kinds of T-cell lymphoma. H9 is a cell line of cutaneous lymphoma with low CD7 expression (Fig. S8A) [32]. Here we determined that three CD7^{KO} CAR-T cells had strong killing activity against H9 cells and there was no obvious difference among them (Fig. S8B). Cytokine secretion levels of three CD7^{KO} CAR-T cells upon H9 stimulation were different, but the differences were within 30% for IFN- γ and within 10% for TNF- α and IL-2 (Fig. S8C). These results indicated robust effector functions of three CD7^{KO} CAR-T cells to different T malignancy-derived cell lines.

Anti-tumor activity of CD7^{KO} CAR-T cells against primary T-ALL blasts

In addition to tumor cell lines, we further evaluated whether CD7^{KO} CAR-T cells could kill primary tumors. Freshly thawed mononuclear leukocytes from bone marrows of two T-ALL patients were first stained to check their CD7 expression. Both samples showed nearly 90% of CD7-positive cells, but tumor cells from patient 2 had higher CD7 expression than those from patient 1 (Fig. 3A). To quantify the ability of CD7^{KO} CAR-T cells to eradicate primary T-blast cells, we co-cultured CAR-T cells with tumor cells at designated E/T ratios and then the number of remaining tumor cells was counted by flow cytometry at indicated time points. Tumor samples were labeled by cell dye before co-culture to clearly distinguish them from CAR-T cells. The results showed that all three CD7^{KO} CAR-T cells were highly effective against primary T-ALL cells derived from both patients (Fig. 3B, C). When CAR-T cells and T-ALL derived from patient 2 were co-cultured at a ratio of 2:1, about 95% of T-ALL cells were eliminated after 48 h. Though with no statistical difference, the average live T-ALL cell numbers of the CD7^{KO&KI}EF1 α group is the lowest and that of the CD7^{KO}TRAC^{KI} group is the highest. Reducing CAR-T dose to 1:1 ratio and co-culture time to 24 h, still nearly 90%, 85%, and 90% T-ALL from both patients killed by CD7^{KO}RV, CD7^{KO}TRAC^{KI}, and CD7^{KO&KI}EF1 α CAR-T cells, respectively, demonstrating the robust effector function of these CAR-T cells against primary tumors.

Two types of site-specific knockin CAR-T cells were more protective in mouse xenograft models of T-ALL

To test *in vivo* anti-tumor function of three CD7-specific CAR-T cells, we used a T-ALL mouse model by engrafting immunodeficient mice intravenously with Jurkat cells engineered to express FFLuc-GFP (firefly luciferase-GFP). A single low dose (1×10^6) of three types of CAR-T cells or untransduced T cells were injected into the mice separately 4 days after tumor seeding to compare the effectiveness of different CAR-T cells (Fig. 4A). The CAR expression levels and CD4/CD8 ratio were determined before injection (Fig. S9). Tumor burdens were monitored by weekly bioluminescent imaging (Fig. 4B, C, E). Compared to untransduced T cells, all three CD7 CAR-T cells could delay T-ALL progression and

extend the median survival of the mice (Fig. 4B–E). More specifically, mice treated with site-specific knockin CAR-T cells, either CD7^{KO}TRAC^{KI} or CD7^{KO&KI}EF1 α cells, showed longer median survival than those treated with retrovirally transduced CAR-T cells (52 days in the CD7^{KO}TRAC^{KI} group, 54 days in the CD7^{KO&KI}EF1 α group vs 44 days in the CD7^{KO}RV group) (Fig. 4D). The result that TRAC^{KI} CAR-T cells performed better than RV CAR-T cells was consistent with the previous study of CD19 CAR-T cells [28]. Intriguingly, in this case, CD7^{KO&KI}EF1 α seemed even better. Though there's no statistical difference between the tumor burdens of CD7^{KO}TRAC^{KI} and CD7^{KO&KI}EF1 α groups, the overall tumor eradication of the CD7^{KO&KI}EF1 α group was slightly superior (Fig. 4B, E). Considering that CD7^{KO&KI}EF1 α only needed one gRNA during manufacturing and had better *in vitro* expansion (Fig. 2E, S5B), the 2-in-1 CD7^{KO&KI} strategy may be a cost-effective choice for making site-specific knockin CD7-specific CAR-T cells. CD7^{KO}RV CAR-T cells seemed to have minimal anti-tumor activity at the low dose (1×10^6). To validate the therapeutic function of CD7^{KO}RV CAR-T cells, we used a higher dose (2×10^6) to see whether a larger cell quantity would compensate for its poor efficacy. Indeed, the higher dose significantly enhanced anti-tumor activities and narrowed the gap between CD7^{KO}RV and CD7^{KO&KI}EF1 α CAR-T cells (Fig. S10A–C). Higher dose also significantly prolonged the median survival of the mice in both groups (Fig. S10D). Therefore, we concluded that even though all three kinds of CAR-T cells in our design have therapeutic potency against T-ALL, the CD7^{KO&KI}EF1 α , and CD7^{KO}TRAC^{KI} strategies significantly enhanced the *in vivo* anti-tumor activities of CD7-specific CAR-T cells in the low dose condition.

CD7^{KO&KI}EF1 α and CD7^{KO}RV CAR-T cells performed very similarly *in vitro* but the former had better anti-tumor activity in Jurkat xenograft models. To further investigate this, we analyzed the CAR-T persistence and expansion *in vivo*. We compared the numbers of CAR⁺ cells in mouse blood, spleen and bone marrow at indicated time points (Fig. S11). Even though no statistical difference was detected due to big individual variation, there was a trend of higher number of CD7^{KO&KI}EF1 α CAR-T cells than that of CD7^{KO}RV. After we conducted a detailed *in vitro* analysis to compare the repeated stimulation-induced exhaustion and expansion of the two kinds of CAR-T cells, we found that CD7^{KO}RV CAR-T cells displayed more exhaustion markers and maintained a relatively higher surface CAR level (Fig. S12). When we monitored the long-term expansion of CAR-T cells upon repeated target stimulation (Fig. S13A), the cell number of CD7^{KO&KI}EF1 α CAR-T increased more than CD7^{KO}RV CAR-T in two independent donors (Fig. S13B). The above observations may explain the better *in vivo* anti-tumor activity of CD7^{KO&KI}EF1 α CAR-T cells.

In addition to Jurkat xenograft models, we also evaluated our CAR-T cells in a second T-ALL model by inoculating with CCRF-CEM cells [18, 21, 24, 33], which are usually harder to control (Fig. S14B). CCRF-CEM had a higher surficial CD7 level than Jurkat (Fig. S14A) and induced higher levels of cytokine secretion (Fig. S14C). Our results showed CCRF-CEM was much harder to kill than Jurkat *in vitro* (Fig. S14B). CCRF-CEM was also much harder to control than Jurkat in mouse models when both treated with 1×10^6 CAR-T cells (Fig. S14D, E). At this dose, CCRF-CEM tumors in both CD7^{KO&KI}EF1 α and CD7^{KO}RV groups grew rapidly with no obvious difference. After the dose was increased to 6×10^6 , tumor growth could be suppressed, confirming the efficacy of CD7^{KO&KI}EF1 α CAR-T cells (Fig. S14F).

To further investigate the contribution of CD7 locus integration and the EF1 α promoter of CD7^{KO&KI}EF1 α CAR-T, we generated two additional types of CAR-T cells. First, CAR was transduced by a lentiviral vector harboring an EF1 α promoter in CD7^{KO} cells, named as CD7^{KO}LV; second, CAR was integrated into the CD7 locus but driven by the LTR promoter that was the same as the promoter in CD7^{KO}RV, named as CD7^{KO&KI}LTR. CAR expression data showed that the LTR promoter performed quite differently in

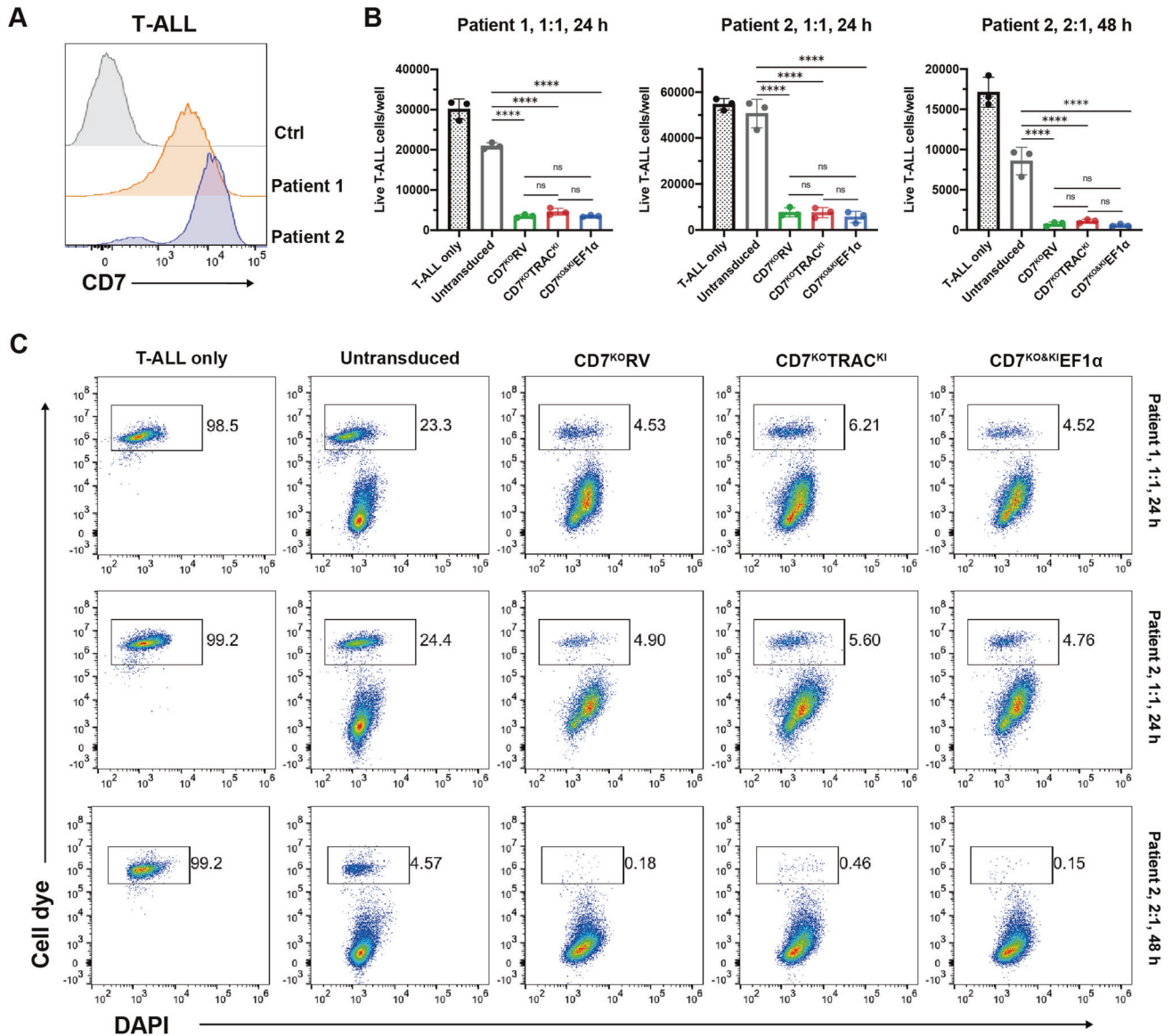


Fig. 3 Anti-tumor activity of CD7^{KO} CAR-T cells against primary T-ALL blasts. **A** Representative histogram showing surface expression of CD7 in two T-ALL patient tumor samples. Ctrl, unstained control. **B** Absolute cell counts of live T-ALL cells quantified by flow cytometry at the end of co-culture. Left, Patient 1 samples, E:T = 1:1, 24 h; middle, Patient 2 samples, E:T = 1:1, 24 h; right, Patient 2 samples, E:T = 2:1, 48 h. **C** Representative dot plots showing frequencies of live T-ALL blasts at the end of co-culture. Top, Patient 1 samples, E:T = 1:1, 24 h; middle, Patient 2 samples, E:T = 1:1, 24 h; bottom, Patient 2 samples, E:T = 2:1, 48 h.

different cassettes. LTR showed particularly strong promoter activity when inserted at the *CD7* locus, leading to high CAR levels in CD7^{KO&KI} LTR CAR-T (Fig. S15A, B). Then we compared four kinds of CAR-T cells side by side (Fig. S15). Even though all four of them showed similar cytotoxicity to Jurkat in vitro (Fig. S15C), they had different therapeutic effects in vivo (Fig. S15D, E). The CD7^{KO&KI}EF1 α CAR-T showed the best anti-tumor effect, and it was followed by CD7^{KO}LV and CD7^{KO}RV CAR-T, respectively. CD7^{KO&KI} LTR CAR-T showed the worst in vivo efficacy, with limited tumor control from the very beginning. Therefore, it appears CAR inserted at the *CD7* locus controlled by the EF1 α promoter had the best therapeutic effect.

Target downregulation is a common cause of tumor escape. Here, we also examined the CD7 expression level in resistant and relapsed tumors (Fig. S16). Cells from the bone marrow of sacrificed mice that had significant tumor burdens (resistant or relapsed) were collected and examined for CD7 expression by FACS (Fig. S16A, B). Compared to tumor cells before injection, the

resistant/relapsed tumor had both a lower percentage of CD7⁺ cells and lower CD7 expression levels (Fig. S16C, D), which indicated tumor cells might escape killing from CAR-T cells by downregulating the surface antigen. Patients with CD7 negative relapse were also reported in some CD7-CAR-T clinical trials [34, 35].

The 2-in-1 strategy generated CAR-NK cells with antitumor activity

When isolating autologous T cells to manufacture CAR-T cells against T cell malignancies, it was hard to distinguish healthy T cells from malignant ones, which can cause product contamination. Using NK cells expressing distinctive surface markers from T cells as an alternative cell source for CAR engineering can largely avoid this issue, as NK cells can be effectively isolated from T cells. However, NK cells also express CD7 (Fig. 5A), which can cause fratricide of CAR-NK cells. Herein, we tried to engineer CD7-specific CAR-NK using the same 2-in-1 CD7^{KO&KI} strategy. TRAC^{KI}

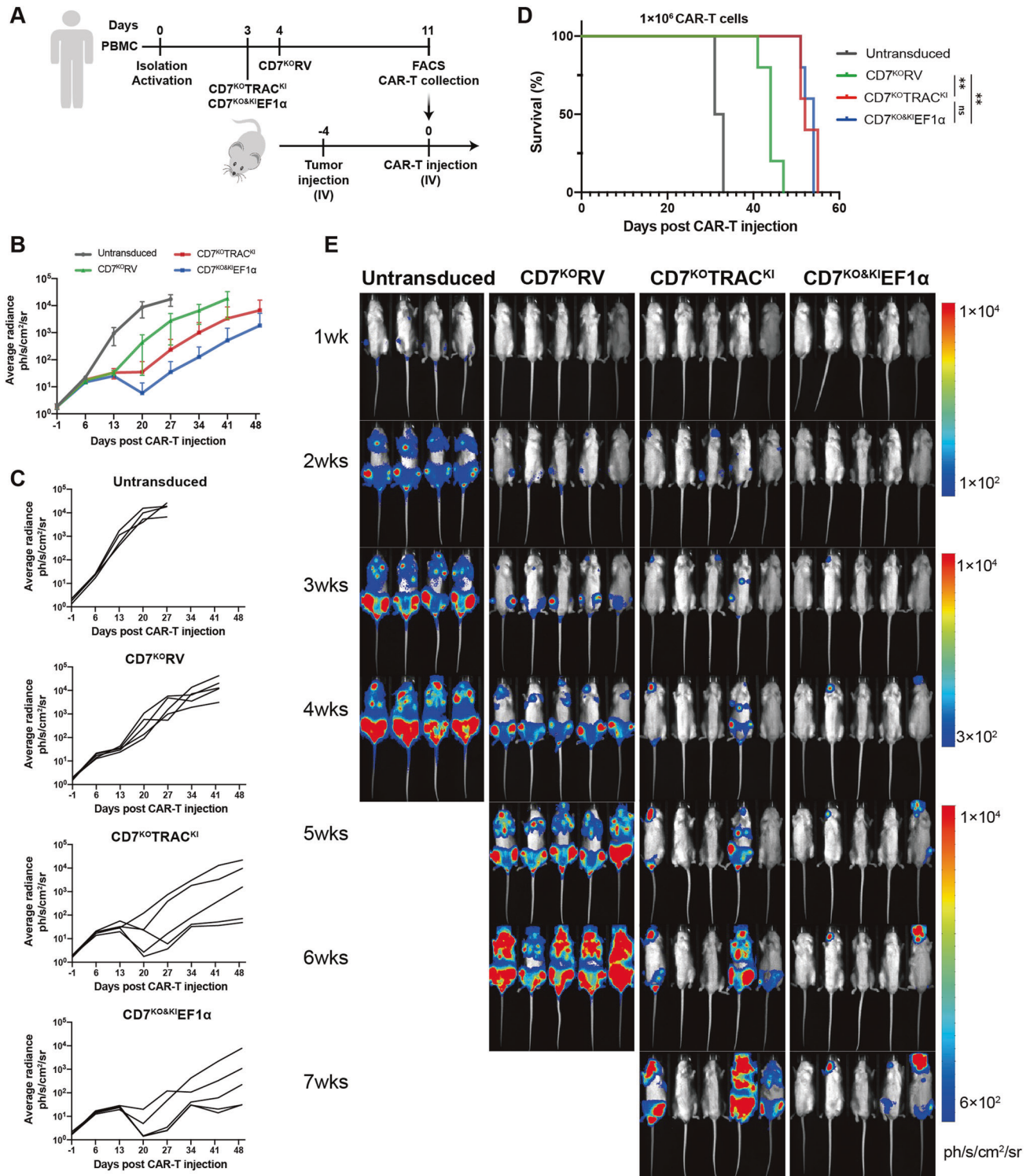


Fig. 4 $CD7^{KO}$ CAR-T cells control the progression of T-ALL in the mouse xenograft model. **A** General outline of the experiment. **B** Average tumor burden (average radiance) of Jurkat-bearing mice treated with 1×10^6 CAR-T cells or equal number of untransduced T cells ($n = 4$ or 5 per group). **C** Tumor burden (average radiance) of Jurkat-bearing mice treated with 1×10^6 CAR-T cells and equal cell number of untransduced T cells ($n = 4-5$; each line tracks one mouse). **D** Kaplan-Meier survival curve of mice injected with untransduced T or CAR-T cells. **E** Bioluminescent images of FFLuc-GFP Jurkat-bearing mice treated with untransduced T or CAR-T cells at indicated days (CAR-T cells were injected at day 0).

strategy was not adopted for CAR-NK because NK cells don't express TCR. NK cells were isolated from PBMC using CD56 beads and then activated by irradiated K562 cells with membrane-bound IL21 and 4-1BBL. CD7 knockout and CAR gene delivery

conducted on Day 4 produced a high percentage of CAR⁺ NK cells (Figs. 5A, S17A). The residual CD7⁺ NK cells were eliminated by CAR⁺ cells as observed in CAR-T cells (Figs. 5A, 2B). Compared to untransduced NK, CD7^{KO&KI}EF1 α CAR-NK exhibited similarly strong

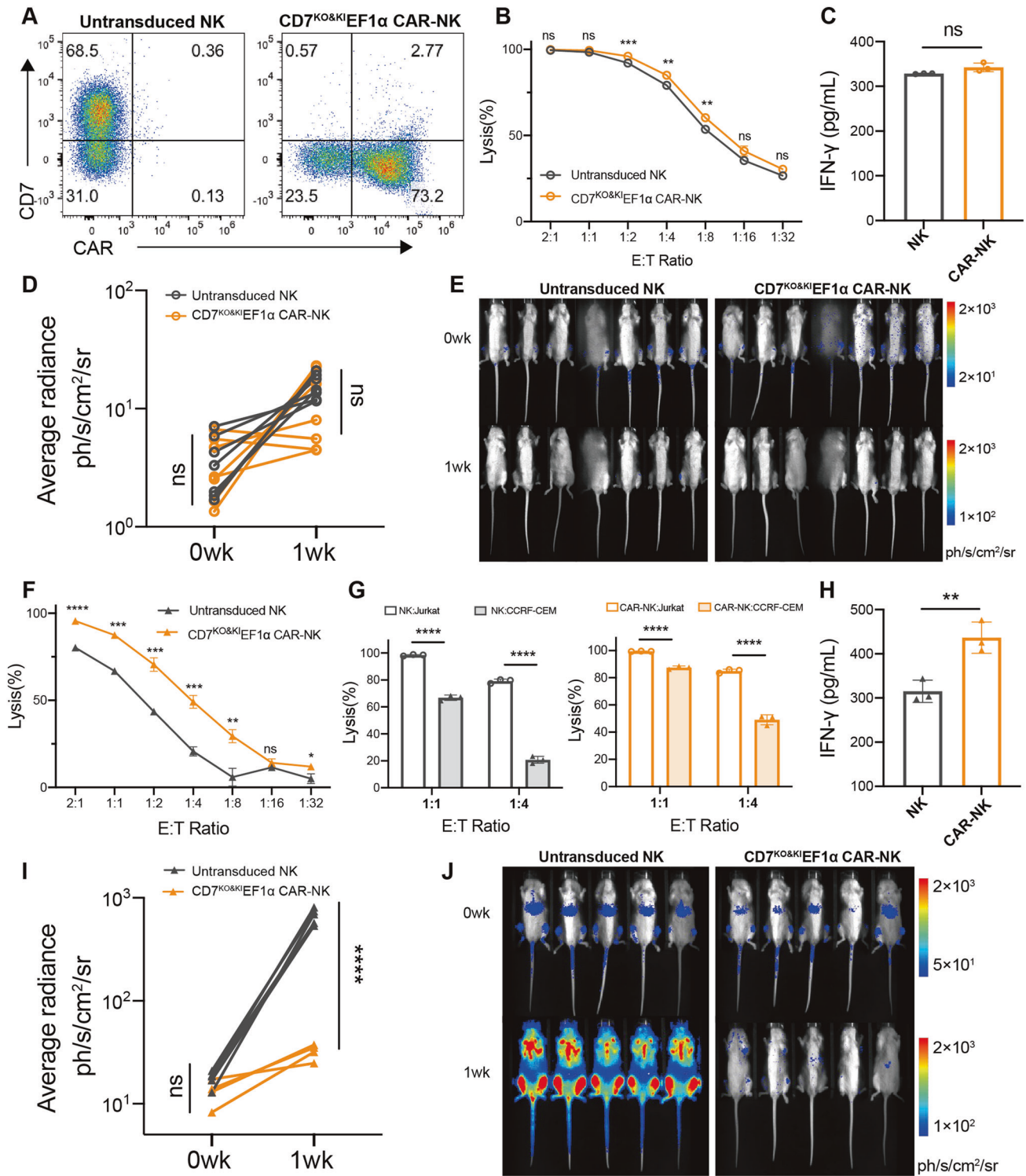


Fig. 5 The 2-in-1 strategy generated CAR-NK cells with anti-tumor activity. **A** Representative dot plots showing surface expression of CD7 and CD7-specific CAR in NK and CAR-NK cells. Numbers indicate the percentage of cells in each quadrant. **B** Cytotoxicity assay of NK and CAR-NK against Jurkat target cells ($n = 3$, mean \pm s.d.). **C** NK and CAR-NK cells were co-cultured with Jurkat cells for 24 h. The IFN- γ secretion in the supernatant was evaluated using CBA kit and FACS ($n = 3$, mean \pm s.d.). **D** Tumor burden (average radiance) of FFLuc-GFP Jurkat-bearing mice before and after 5×10^6 NK or CAR-NK cells administration (each line tracks one mouse; 0wk data gathered a day before NK/CAR-NK cells administration). **E** Bioluminescent images of FFLuc-GFP Jurkat-bearing mice before and after NK/CAR-NK cells treatment. **F** Cytotoxicity assay of NK and CAR-NK against CCRF-CEM target cells ($n = 3$, mean \pm s.d.). **G** The differences between lysis efficiency of NK (left)/CAR-NK (right) to Jurkat and to CCRF-CEM. **H** NK and CAR-NK cells were co-cultured with CCRF-CEM cells for 24 h. The IFN- γ secretion in the supernatant was evaluated using CBA kit and FACS ($n = 3$, mean \pm s.d.). **I** Tumor burden (average radiance) of FFLuc-GFP CCRF-CEM-bearing mice before and after 2.5×10^7 NK or CAR-NK cells administration (each line tracks one mouse; 0wk data gathered a day before NK/CAR-NK cells administration). **J** Bioluminescent images of FFLuc-GFP CCRF-CEM-bearing mice before and after NK/CAR-NK cells treatment.

cytotoxicity to Jurkat cells in a 4-hour in vitro killing assay (Fig. 5B). The INF- γ secretion after Jurkat stimulation was also similar (Fig. 5C). In vivo experiments showed that CAR-NK and untransduced NK had similar anti Jurkat tumor activities at both a low (5×10^6) and a high (5×10^7) dosage (Figs. 5D, E, S17B). As Jurkat is a T-ALL line relatively easy to kill, we further evaluated CD7^{KO&KI}EF1 α CAR-NK in CCRF-CEM models, which are harder to control (Fig. 5F–J). Similar to the outcomes in CAR-T cells, CCRF-CEM was also harder to kill than Jurkat by both NK and CAR-NK cells (Fig. 5G). And CD7^{KO&KI}EF1 α CAR-NK were superior to untransduced NK in treating CCRF-CEM tumors in terms of cytotoxicity, cytokine secretion and in vivo anti-tumor activity (Figs. 5F, H, I, J, 17C), indicating our 2-in-1 CD7^{KO&KI} strategy is capable of producing effective CAR-NK cells.

Therefore, our design to place EF1 α -driven CD7 CAR directly at the CD7 locus is a feasible strategy that is effective in both T and NK cells. Additionally, such 2-in-1 strategy is also applicable for CAR-T and CAR-NK cells targeting other T-cell antigens, such as CD5.

DISCUSSION

Recently, as CAR-T therapy revolutionized the treatment of B-cell malignancies, studies focusing on CD7-specific CAR-T cells are booming. Dozens of products are being evaluated in clinical trials to treat T cell-derived leukemia and lymphoma, showing promising tumor remission in the early-stage results [14, 16, 17]. It is worthy of note that the candidate antibody clone T3-3A1 used as a T cell probe and in CD7 ADCs, is believed to bind specifically to CD7⁺ cells [9, 30]. Nevertheless, in our CAR construct, using T3-3A1 as an antigen recognition domain failed to activate CAR-T cells upon antigen stimulation. CAR signaling could be affected by multiple factors, such as antigen binding affinity and epitope position [36, 37]. Thus, standards differ from therapeutic antibody screening are needed to select scFv sequences for CAR. Therefore, testing CAR designs in primary T cells is still the most effective and direct way.

To reduce the fratricide of CD7-specific CAR-T cells, we developed a 2-in-1 strategy where an EF1 α -driven CD7-specific CAR was inserted at the knocked-out CD7 locus. And we compared it to two other known strategies, one was random integration of CAR by a retrovirus and the other was site-specific integration at the TRAC locus by gene editing. CD7^{KO}TRAC^{KI}, CD7^{KO&KI}EF1 α CAR-T cells based on site-specific integration showed a similar response to antigen stimulation as retrovirus-transduced CD7^{KO}RV CAR-T cells in vitro. All of them displayed strong cytotoxicity to both T-leukemia and lymphoma cell lines, as well as primary tumor cells from patients. Moreover, TRAC^{KI} and CD7^{KI}EF1 α CAR-T cells exhibited enhanced tumor rejection in a mouse xenograft model of T-ALL compared with RV cells, demonstrating the potential of site-specific CD7 CAR-T cells for clinical application. As producing CD7^{KO}TRAC^{KI} CAR-T cells uses more gRNA types and larger amounts of ribonucleoproteins (RNPs) than the 2-in-1 strategy, it is likely to cause higher off-target risk, lower expansion and higher costs. More importantly, the 2-in-1 target knockout and CAR knockin strategy we presented could be widely applicable to CARs specific for other targets expressed on T cells, such as CD5. Thus CD7^{KO&KI} should be a better strategy than CD7^{KO}TRAC^{KI} for autologous site-specific CD7 CAR-T products. It is also important to note that a well-matched promoter is a prerequisite for the ideal therapeutic effects of CD7^{KO&KI} CAR-T (Fig. S15). Additionally, in a different scenario of producing universal CAR-T cells from allogeneic T cells where TCR needs to be disrupted to prevent graft-versus-host disease (GVHD) [38], target knockout and CAR knockin at TRAC locus might be a better solution.

TRAC^{KI} CD19-specific CAR-T cells reported by Eyquem et al. had minimal tonic signaling because of low CAR expression and CAR

downregulation upon antigen stimulation, thus resulting in less exhausted cells and better tumor control. Similarly, in our results, CD7^{KO}TRAC^{KI} CAR-T cells displayed lower CAR MFI and better tumor rejection than CD7^{KO}RV CAR-T cells. In the previous study, TRAC^{KI} CD19 CAR under EF1 α control made T cells express higher CAR but showed inferior in vivo anti-tumor activity than TRAC^{KI} CD19 CAR under TRAC intrinsic promoter control [28]. However, CD7^{KI} CAR under EF1 α control in our results showed a similar expression level as well as tumor control to TRAC^{KI} CAR under TRAC intrinsic promoter control. The observation that the same EF1 α promoter in different genomic sites may lead to different expression levels suggested that transgene expression could be regulated by both integration locus and exogenous promoter. Such phenomenon was even more obvious in terms of the LTR promoter (Fig. S15).

Furthermore, the 2-in-1 CD7^{KO&KI} also can be extended to CAR-NK production as NK cells also express CD7 causing fratricide. However, CD7^{KO&KI}EF1 α CAR-NK cells showed similar anti-tumor activity to Jurkat cells as untransduced NK cells. It is likely because Jurkat is usually easy to kill and untransduced NK cells already have enough capability to control it. Whereas, in a different evaluation model, CCRF-CEM, CD7^{KO&KI}EF1 α CAR significantly improved the anti-tumor activities of NK cells.

In conclusion, our 2-in-1 knockout and knockin strategy expressing CD7 CAR from the CD7 locus under the control of EF1 α promoter reduces fratricide and enhances tumor rejection against T-ALL in CAR-T and CAR-NK cells. To develop autologous CD7-specific CAR-T cells, CD7^{KO&KI} is recommended as a cost-effective and lower-risk choice; to develop universal products, CD7^{KO}TRAC^{KI} is also a practical choice for CAR-T as TRAC can be disrupted to prevent GVHD while CD7^{KO&KI} is applicable to produce CAR-NK.

METHODS

Isolation and expansion of human T cells and NK cells

Human peripheral blood mononuclear cells (PBMCs) were isolated from the peripheral blood of healthy volunteers using the Human Lymphocyte Separation Medium (Dakewe). Ethical permission was granted by the School of Medicine, Zhejiang University. Informed consent was obtained from all donors. All blood samples were handled following the required ethical and safety procedures. T cells were isolated from PBMCs using the Pan T Cell Isolation Kit (Miltenyi Biotec), and then stimulated with CD3/CD28 T cell Activator Dynabeads (ThermoFisher) for 48 h. X-VIVO 15 Serum-free Hematopoietic Cell Medium (Lonza) supplemented with 10% fetal bovine serum (Vistech), 1% penicillin/streptomycin (Gibco), 5 ng/ml interleukin-7 (IL-7) and 5 ng/ml interleukin-15 (IL-15) (Novoprotein) were used to cultivate T cells. NK cells were isolated from PBMCs using CD56⁺ selection kit (Miltenyi Biotec) and then stimulated with irradiated K562 with membrane-bound IL21 and 4-1BBL. Cell debris were removed by density gradient centrifugation on Day3 after activation. RPMI1640 (BasalMedia) supplemented with 10% fetal bovine serum (Vistech), 1% penicillin/streptomycin (Gibco), 5 ng/ml interleukin-15 (IL-15) (Novoprotein) and 200 ng/ml interleukin-2 (IL-2) (Novoprotein) were used to cultivate NK cells.

gRNA sequence

TRAC gRNA: 5'-C* A* G*GGUUCUGGAUAUCUGUGUUUAGAGCUAG AAAUAGCAAGUUAAAAUAAGGCUAGUCCGUUAUCAACUUGAAAAAGUG GCACCGAGUCGGUGUCU* U* U* U-3'
 CD7 gRNA: 5'-G*G*A*GCAGGUGAUGUUGACGGGUUUUAGAGCUAG AAAUAGCAAGUUAAAAUAAGGCUAGUCCGUUAUCAACUUGAAAAAGUGG CACCGAGUCGGUGUCU*U*U* U -3'. Asterisk (*) represents 2' -O-methyl 3' phosphorothioate.

CAR design and gene targeting

Sequences of three CD7-specific single-chain variable fragments were obtained from CN2017800730716A and created using commercial gene synthesis. Plasmids encoding CD7-specific CARs were constructed by inserting CAR constructs into SFG γ -retroviral vector, lentiviral vector or

AAV vector that were previously used [28]. 48 h after initiating T-cell activation, the CD3/CD28 beads were magnetically removed, and the next day the T cells were transfected by electrotransfer of RNPs. In detail, 1×10^9 cells were mixed with 60 pmol gRNA and 6 μ g Cas9 protein in a total volume of 120 μ L and then transferred to a 120 μ L cuvette and electroporated with a Cell Electroporator (CELETRIX). For site-specific knockin CAR-T, AAV virus (MOI = 1×10^9) (Vigene Biosciences, China) were added 20 min after electroporation. For random integrated CAR-T, retroviruses or lentiviruses were produced from 293T cell lines and T cells were transduced with retroviral/lentiviral supernatants by centrifugation on retronectin (Takara)-coated plates on the next day.

Flow cytometry

The following fluorophore-conjugated antibodies were used: Alexa Fluor 647 anti-HA.11 Epitope Tag (#682404) from Biologend; Anti-Hu CD7-Alexa Fluor 700 (#56-0079-42), Anti-Human CD4-Super Bright 645 (#2094166), Anti-Human CD8a-PE (#2361080), Anti-Human CD62L-eFluor 450 (#48-0629-42) and Anti-Human CD45RA-eFluor 506 (#69-0458-42) from Invitrogen; PE Mouse Anti-Human CD3 from BD Pharmingen. Cytometry data were obtained in a CytoFLEX (Beckman) and Data analysis was performed using FlowJo software.

Genome PCR

CAR-T cells were harvested 8 days after gene targeting for DNA extraction by FastPure cell/Tissue DNA Isolation Mini kit (Vazyme). The TRAC locus target sequences were amplified with Taq DNA polymerase (Vazyme) with forward primer-F (GCAGTATTATTAAGTAGCCC) and reverse primer-R (GTGGCAATGGATAAGGCCGA). The CD7 locus target sequences were amplified with Taq DNA polymerase (Vazyme) with forward primer-F (GTGCTGAGCGGCTCC) and reverse primer-R (GGACATGTAGGAGGGAG).

Cell viability and cell number assay

A mixture of acridine orange and propidium iodide was used to stain viable and dead cells. Cell number and cell viability were then recorded by a Countstar Rigel S3 Fluorescence Cell Analyzer (Countstar).

Cytotoxicity assay

Tumor cell lines Jurkat cells (from National Collection of Authenticated Cell Cultures), CCRF-CEM cells (from National Collection of Authenticated Cell Cultures) and H9 cells [32] were transduced to express firefly luciferase (FFLuc)-GFP, cultured in complete RPMI1640 (BasalMedia) with 10% fetal bovine serum (FBS, Vistech) and 1% penicillin/streptomycin (Gibco). For luciferase-based cytotoxicity assay, the effector(E) and target(T) cells were co-cultured in triplicates at indicated E/T ratios using black 96-well flat plates (WHB) with 5×10^4 target cells in a total volume of 100 μ L per well in RPMI1640 medium. Target cells alone were plated at the same cell density to determine the maximal luciferase expression (relative light units; RLU_{max}). 18 h (for CAR-T) /4 h (for CAR-NK) later, 100 μ L luciferase substrate (Perkin) was added to each well. Emitted light was detected in a luminescence plate reader (ThermoFisher). Lysis was determined as $(1 - (RLU_{\text{sample}}/RLU_{\text{max}})) \times 100\%$.

Antigen stimulation and cytokines analysis assay

CAR-T/CAR-NK cells were co-cultured with target cells at a ratio of 4:1 without the addition of exogenous cytokines for 24 h, then culture supernatants were harvested and analyzed using a BD CBA Human Soluble Protein Master Buffer Kit (BD Biosciences) according to the manufacturer's instructions. The detection reagent is a mixture of phycoerythrin (PE)-conjugated antibodies, which provides a fluorescent signal in proportion to the amount of bound analyte. Soluble cytokine can be measured using flow cytometry to identify particles with fluorescence characteristics of both the bead and the detector.

CFSE-based proliferation assay

For CFSE-based proliferation assay, CAR-T cells were labeled with cell dye using CytoTell™ Orange from AAT Bioquest. Briefly, cells were resuspended in D-PBS (GENOM) at a final concentration of 1×10^6 cells/mL, cell dye solution was added at the suggested working concentration. The CAR-T cells were incubated at 37 °C for 15 min, and then washed three times with D-PBS. Labeled cells were further plated in 24-well plates in the absence or presence of Jurkat cells (E:T = 4:1). 96 h later, cells were harvested and analyzed by CytoFLEX (Beckman) with FlowJo software (FlowJo 10.4).

In vitro primary T-ALL killing assay

Mononuclear leukocytes from bone marrow of two T-ALL patients were obtained from The Children's Hospital, Zhejiang University School of Medicine. The protocol for collection of bone marrow from T-ALL patients was approved by The Children's Hospital, Zhejiang University School of Medicine. Primary tumor cells were isolated from bone marrow samples using Human Lymphocyte Separation Medium and labeled with CytoTell™ Orange cell dye (AAT Bioquest). Labeled tumor cells were then co-cultured with CAR-T cells or unmodified T cells for 24 h or 48 h at a 1:1 or 2:1 ratio before FACS analysis. DAPI (Beyotime) was added to discriminate live cells from dead cells, and Counting Beads (Invitrogen) were added to quantify the absolute cell counts of live tumor cells.

Xenograft models

6–10 weeks old NSPG (Jihui) mice were used. All mice were housed at the Westlake University under pathogen-free conditions, and all procedures were approved by the ethical committee of Westlake University. Jurkat/CCRF-CEM cells transduced with luciferase were injected by tail vein at a total number of 5×10^5 per mouse 4 days before therapeutic cells injection. Tumor burden was measured by bioluminescence imaging using Biospace Optima small animal imaging system (Biospace Lab) at indicated time points. M3 vision software was used to visualize and calculate average luminescence. Mice were selected and assigned to groups randomly before T/NK injection.

Isolation of cells from blood, bone marrow, and spleen

Mice were euthanized with CO₂ at day 71 after 2×10^6 CAR-T cells administration. Bone marrow was harvested from freshly isolated femurs and tibiae. After removal of connective tissues and muscles, bones and spleens were crushed in 5 mL PBS with 0.5% BSA. Single-cell suspensions were made by pipetting and passing supernatant from bone marrow and spleen through a 40 μ m filter (BD Falcon). Blood was collected from the submandibular vein. RBCs were lysed using ACK buffer before FACS analysis (Solarbio).

Statistical analysis

Student *t* test or One-way ANOVA was carried out using GraphPad Prism version 8.0 (GraphPad Software Inc). ns, $P > 0.05$; *, $P < 0.05$; **, $P < 0.01$; ***, $P < 0.001$ and ****, $P < 0.0001$.

AVAILABILITY OF DATA AND MATERIALS

All data obtained and/or analyzed during the current study are available from the corresponding authors on reasonable request.

REFERENCES

- June CH, Sadelain M. Chimeric antigen receptor therapy. *N Engl J Med.* 2018;379:64–73.
- Park JH, Riviere I, Gonen M, Wang X, Senecal B, Curran KJ, et al. Long-term follow-up of CD19 CAR therapy in acute lymphoblastic leukemia. *N Engl J Med.* 2018;378:449–59.
- Raje N, Berdeja J, Lin Y, Siegel D, Jagannath S, Madduri D, et al. Anti-BCMA CAR T-cell therapy bb2121 in relapsed or refractory multiple myeloma. *N Engl J Med.* 2019;380:1726–37.
- Fleischer LC, Spencer HT, Raikar SS. Targeting T cell malignancies using CAR-based immunotherapy: challenges and potential solutions. *J Hematol Oncol.* 2019;12:141.
- Ware RE, Scarse RM, Dietz MA, Starmer CF, Palker TJ, Haynes BF. Characterization of the surface topography and putative tertiary structure of the human CD7 molecule. *J Immunol.* 1989;143:3632–40.
- Wenzinger C, Williams E, Gru AA. Updates in the pathology of precursor lymphoid neoplasms in the revised fourth edition of the who classification of tumors of hematopoietic and lymphoid tissues. *Curr Hematol Malig Rep.* 2018;13:275–88.
- Baum W, Steininger H, Bair HJ, Becker W, Hansen-Hagge TE, Kressel M, et al. Therapy with CD7 monoclonal antibody TH-69 is highly effective for xenografted human. *Br J Haematol.* 1996;95:327–38.
- Paauz ME, Doumbia SO, Pennell CA. Construction and characterization of human CD7-specific single-chain Fv immunotoxins. *J Immunol.* 1997;158:3259–69.
- Uckun FM, Ramakrishnan S, Houston LL. Immunotoxin-mediated elimination of clonogenic tumor cells in the presence of human bone marrow. *J Immunol.* 1985;134:2010–6.

10. Zhang J, Jain A, Milhas S, Williamson DJ, Mysliwy J, Lodge A, et al. An antibody-drug conjugate with intracellular drug release properties showing specific cytotoxicity against CD7-positive cells. *Leuk Res.* 2021;108:106626.
11. Yu Y, Li J, Zhu X, Tang X, Bao Y, Sun X, et al. Humanized CD7 nanobody-based immunotoxins exhibit promising anti-T-cell acute lymphoblastic leukemia potential. *Int J Nanomed.* 2017;12:1969–83.
12. Brammer JE, Saliba RM, Jorgensen JL, Ledesma C, Gaballa S, Poon M, et al. Multi-center analysis of the effect of T-cell acute lymphoblastic leukemia subtype and minimal residual disease on allogeneic stem cell transplantation outcomes. *Bone Marrow Transpl.* 2017;52:20–7.
13. Litzow MR, Ferrando AA. How I treat T-cell acute lymphoblastic leukemia in adults. *Blood.* 2015;126:833–41.
14. Bayon-Calderon F, Toribio ML, Gonzalez-Garcia S. Facts and challenges in immunotherapy for T-cell acute lymphoblastic leukemia. *Int J Mol Sci.* 2020;21:7685.
15. U.S. National Library of Medicine. ClinicalTrials. <https://clinicaltrials.gov>.
16. Pan J, Tan Y, Wang G, Deng B, Ling Z, Song W, et al. Donor-derived CD7 chimeric antigen receptor T cells for T-cell acute lymphoblastic leukemia: first-in-human, phase I trial. *J Clin Oncol.* 2021;39:3340–52.
17. Teachey DT, Hunger SP. Anti-CD7 CAR T cells for T-ALL: impressive early-stage efficacy. *Nat Rev Clin Oncol.* 2021;18:677–8.
18. Gomes-Silva D, Srinivasan M, Sharma S, Lee CM, Wagner DL, Davis TH, et al. CD7-edited T cells expressing a CD7-specific CAR for the therapy of T-cell malignancies. *Blood* 2017;130:285–96.
19. Mamonkin M, Mukherjee M, Srinivasan M, Sharma S, Gomes-Silva D, Mo F, et al. Reversible transgene expression reduces fratricide and permits 4-1BB costimulation of CAR T cells directed to T-cell malignancies. *Cancer Immunol Res.* 2018;6:47–58.
20. Rasaiyaah J, Georgiadis C, Preece R, Mock U, Qasim W. TCR α beta/CD3 disruption enables CD3-specific antileukemic T cell immunotherapy. *JCI Insight.* 2018;3:e99442.
21. Cooper ML, Choi J, Staser K, Ritchey JK, Devenport JM, Eckardt K, et al. An “off-the-shelf” fratricide-resistant CAR-T for the treatment of T cell hematologic malignancies. *Leukemia* 2018;32:1970–83.
22. Georgiadis C, Rasaiyaah J, Gkazi SA, Preece R, Etuk A, Christi A, et al. Base-edited CAR T cells for combinational therapy against T cell malignancies. *Leukemia.* 2021;35:3466–81.
23. Gomes-Silva D, Atilla E, Atilla PA, Mo F, Tashiro H, Srinivasan M, et al. CD7 CAR T Cells for the therapy of acute myeloid leukemia. *Mol Ther.* 2019;27:272–80.
24. Png YT, Vinanica N, Kamiya T, Shimasaki N, Coustan-Smith E, Campana D. Blockade of CD7 expression in T cells for effective chimeric antigen receptor targeting of T-cell malignancies. *Blood Adv.* 2017;1:2348–60.
25. Freiwan A, Zoine J, Crawford JC, Vaidya A, Schattgen SA, Myers J, et al. Engineering naturally occurring CD7 negative T cells for the immunotherapy of hematological malignancies. *Blood* 2022;140:2684–96.
26. Wang X, Riviere I. Clinical manufacturing of CAR T cells: foundation of a promising therapy. *Mol Ther Oncol.* 2016;3:16015.
27. Ellis DJ. Silencing and variegation of gammaretrovirus and lentivirus vectors. *Hum Gene Ther.* 2005;16:1241–6.
28. Eyquem J, Mansilla-Soto J, Giavridis T, van der Stegen SJ, Hamieh M, Cunanan KM, et al. Targeting a CAR to the TRAC locus with CRISPR/Cas9 enhances tumour rejection. *Nature.* 2017;543:113–7.
29. Melenhorst JJ, Chen GM, Wang M, Porter DL, Chen C, Collins MA, et al. Decade-long leukaemia remissions with persistence of CD4(+) CAR T cells. *Nature.* 2022;602:503–9.
30. Mayer KE, Mall S, Yusufi N, Gosmann D, Steiger K, Russell L, et al. T-cell functionality testing is highly relevant to developing novel immuno-tracers monitoring T cells in the context of immunotherapies and revealed CD7 as an attractive target. *Theranostics.* 2018;8:6070–87.
31. Gattinoni L, Lugli E, Ji Y, Pos Z, Paulos CM, Quigley MF, et al. A human memory T cell subset with stem cell-like properties. *Nat Med.* 2011;17:1290–7.
32. Gu Y, Zhang J, Ma X, Kim BW, Wang H, Li J, et al. Stabilization of the c-Myc protein by CAMKII γ promotes T cell lymphoma. *Cancer Cell.* 2017;32:115–28.
33. Lu P, Liu Y, Yang J, Zhang X, Yang X, Wang H, et al. Naturally selected CD7 CAR-T therapy without genetic manipulations for T-ALL/LBL: first-in-human phase I clinical trial. *Blood.* 2022;140:321–34.
34. Pan J, Tan Y, Wang G, Deng B, Ling Z, Song W, et al. Donor-derived CD7 chimeric antigen receptor T cells for T-cell acute lymphoblastic leukemia: first-in-human, phase I trial. *J Clin Oncol.* 2021;39:3340–51.
35. Tan Y, Shan L, Zhao L, Deng B, Ling Z, Zhang Y, et al. Long-term follow-up of donor-derived CD7 CAR T-cell therapy in patients with T-cell acute lymphoblastic leukemia. *J Hematol Oncol.* 2023;16:34.
36. Duan Y, Chen R, Huang Y, Meng X, Chen J, Liao C, et al. Tuning the ignition of CAR: optimizing the affinity of scFv to improve CAR-T therapy. *Cell Mol Life Sci.* 2021;79:14.
37. Xiao Q, Zhang X, Tu L, Cao J, Hinrichs CS, Su X. Size-dependent activation of CAR-T cells. *Sci Immunol.* 2022;7:eabl3995.
38. Depil S, Duchateau P, Grupp SA, Mufti G, Poirot L. ‘Off-the-shelf’ allogeneic CAR T cells: development and challenges. *Nat Rev Drug Discov.* 2020;19:185–99.

ACKNOWLEDGEMENTS

The authors thank the support of Zhejiang Provincial Key Laboratory of Immunity and Inflammatory Diseases, and thank Yueting Xin, Chun Guo, Jiajia Wang, Yingying Huang from the core facilities, Zhejiang University School of Medicine for their technical support.

AUTHOR CONTRIBUTIONS

JJ and JS designed the studies and conceived the experiments. JJ, JC, and YW performed most of the experiments; CL, DY, KS conducted data analysis; YH, YT, and XG contributed reagents. JJ, YG, and JS wrote the manuscript. YG and JS supervised the study. All authors read and approved the final manuscript.

FUNDING

This research was funded by the National Key R&D Program of China 2021YFA0909900 (JS), 2018YFA0800102 (YG), the National Natural Science Foundation of China grants 31971324 (JS), 31970555 (YG), 82161138028 (JS), 81973993 (XG), Zhejiang Provincial Natural Science Foundation grant LR20H160003 (JS), LR20C070001 (XG) and the Leading Innovative and Entrepreneur Team Introduction Program of Zhejiang grant 2020R01006 (JS, YG).

COMPETING INTERESTS

The authors declare no competing interests.

ETHICS APPROVAL AND CONSENT TO PARTICIPATE

All animal studies were reviewed and approved by the Ethical Committee of Westlake University.

ADDITIONAL INFORMATION

Supplementary information The online version contains supplementary material available at <https://doi.org/10.1038/s41375-023-01948-3>.

Correspondence and requests for materials should be addressed to Ying Gu or Jie Sun.

Reprints and permission information is available at <http://www.nature.com/reprints>

Publisher's note Springer Nature remains neutral with regard to jurisdictional claims in published maps and institutional affiliations.

Springer Nature or its licensor (e.g. a society or other partner) holds exclusive rights to this article under a publishing agreement with the author(s) or other rightsholder(s); author self-archiving of the accepted manuscript version of this article is solely governed by the terms of such publishing agreement and applicable law.